Tutorial

Anna Möhl and Ulrike Fuchs*

Exploring the unlimited possibilities of modular aspheric Gauss to top-hat beam shaping

DOI 10.1515/aot-2016-0030
Received May 4, 2016; accepted June 16, 2016

Abstract: Beam shaping is a field of research with growing importance. Therefore, a new refractive beam shaping system is presented. The knowledge gained from analyzing patent systems was used to derive our own improved design. It is compared to a patent system, and some selected results are presented in this work. Furthermore, possibilities to scale the entrance and exit beam diameters with the help of SPA™ Beam Expander Kit and SPA™ AspheriColl (both from asphericon GmbH, Jena, Germany) are shown, so that a modular top-hat generation is achievable. Additionally, the large spectral range in which the beam shaping system is applicable is demonstrated, and it is demonstrated how the beam shaping system can be used to improve the performance of other optical elements that require a top-hat beam profile.

Keywords: aspheres; optical design top-hat Gauss; refractive beam shaping.

1 Introduction

Many laser applications, especially in the field of material processing, lithography, or optical data storage, require a uniform intensity distribution [watts/area], rather than the well-known Gaussian beam profile of the working beam to guarantee an optimum performance. For this reason, Gauss to top-hat beam shaping is a field of research with growing importance.

To generate a top-hat beam profile, several approaches are already known. They can be divided into three categories: aperture systems, beam integrators, and field mapping systems [1]. In the past, a uniform illumination was generated by expanding a Gaussian beam to be much larger than the area to be illuminated. Just the central region of the beam was used. The outer region of the beam is discarded by a finite aperture. Another approach is to break up the input beam into smaller beamlets that are directed to overlap in the output plane with a desired shape. They often consist of micro-lens arrays [2].

Using apertures and integrators for beam shaping can be rather difficult. These systems are difficult to manufacture and, consequently, are relatively expensive. Additionally, integrators have strong wavelength dependence, and through the use of apertures for beam shaping, a significant energy loss occurs. However, a promising strategy is to use refractive optical elements for beam shaping, as they are very efficient, have a simple structure, are easier to manufacture compared to diffractive solutions, and are more flexible with respect to wavelength changes.

The basic principle of refractive beam shaping, introduced by Frieden and Kreuzer, consists of two rotational symmetric plano-aspheric lenses in a certain distance to each other [3, 4]. The first aspheric surface changes the incoming plane wave with a non-uniform intensity profile by redistributing the rays, so a uniform intensity profile is generated. The task of the second aspheric surface is to recollimate the output beam. According to the working principle, refractive beam shaping systems can be divided into two types: Galilean- and Keplerian-type beam shaping systems. A Keplerian-type beam shaping system consists of two positive lenses. This system has an internal focus. As a consequence of the internal focus, very high intensities can occur in this region. Furthermore, the overall system length cannot fall below a certain value. The Galilean-type beam shaping system has a first lens that is negative. Subsequently, there is no internal focusing in this system and the overall system length can be significantly shorter. This kind of beam shaping system is more suitable for most applications. The Galilean beam shaping systems are considered as basic elements within the modular approach discussed in this article.

***Corresponding author: Ulrike Fuchs,** asphericon GmbH, Stockholmer Str. 9, 07747 Jena, Germany,
e-mail: u.fuchs@asphericon.com
Anna Möhl: asphericon GmbH, Stockholmer Str. 9, 07747 Jena, Germany

Several theoretical designs for refractive beam shaping systems have already been developed and published [5, 6]. Above that, it is very important for the practical application of these systems to guarantee a reproducible and precise fabrication, and controlling the manufacturing costs. Therefore, it was a subject of detailed investigations to analyze a refractive Gauss to top-hat beam shaper, especially to simulate the as-built performance [7]. Furthermore, the stability of the beam shaping system is investigated [8]. In the following, a compact optical design for a refractive beam shaping system, which simultaneously has a high optical performance and can be produced in series reliably, is presented. Furthermore, it is shown that the beam shaping system is applicable with the existing monolithic beam expander kit of asphericon GmbH so that a modular top-hat generation is possible.

2 Set-up of the basic beam shaping system

The main idea for setting up a modular beam shaping concept is a divide-and-conquer approach, which creates three different tasks. The first task is to adapt the incoming beam diameter to the required diameter for the beam shaping process, which is the second task. Last but not least, one needs to be able to scale the output beam diameter to the size needed for the application. Even though there are a few beam shaping systems already commercially available, combining these three basic needs has not been a trivial task so far. Above that, the overall length of such set-ups is usually impractically long. Thus, the superordinate challenge is creating a modular system with minimum overall length without loosening the requirements concerning the beam profile quality. The first member of the modular system discussed is the Gauss to top-hat beam shaping system itself.

The beam shaping system is based on the idea of Kreuzer's patent [4]. Its layout is shown in Figure 1 (top). It is a one-to-one beam shaping system designed for a wavelength of λ=632 nm, an input beam diameter of D=30 mm. The distance between the lenses is L=150 mm and the working distance, in which the top-hat beam profile is generated, is WD=100 mm. The intensity distribution at the working distance of 100 mm, which was generated by the considered beam shaping system with ideal surfaces, is shown in Figure 2 (left, blue dashed line). It can be seen that nearly a perfect top-hat beam profile can be achieved. In order to get a high-quality top-hat beam profile, a maximum slope deviation of the aspheric surfaces in a range of RMS$\Delta S_{2\text{-dim}}$(75 µrad/1/0.1) [root mean square (RMS)] was determined [7, 8]. In Figure 2 (left, solid red line), the intensity distribution at the working distance of 100 mm is simulated for real surfaces of this quality level.

Figure 1 (bottom) shows our optimized optical design, which was derived after analyzing the as-built performance of patent systems. The aim was to keep the optical performance at least at the same level, shorten the overall system length, and create a stable solution with respect to alignment tolerances, which define the way this optical system can be mounted. As this is a beam shaping application, all refractive surfaces are very sensitive to slope deviation. How this influences the propagation behavior of the top-hat distribution is discussed in Refs. [7, 8]. Comparing this new beam shaping system to the system based on Kreuzer's patent, one can notice the reduced entrance beam diameter resulting from the modular approach. Its benefits will be shown in a later section.

Furthermore, it can be seen that the system length of the new design could be reduced by 50%. The length of the patent system is comparable with most of the available

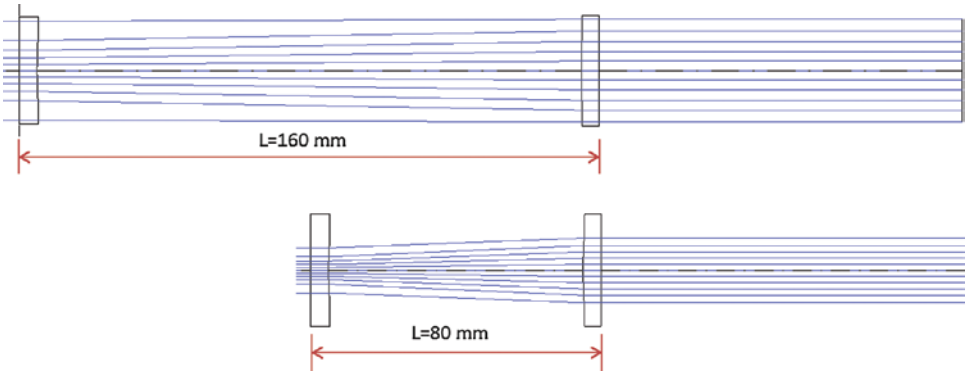

Figure 1: Layout of (top) a simulation of Kreuzer's patent [4] and (bottom) of the optical design derived in Ref. [8].

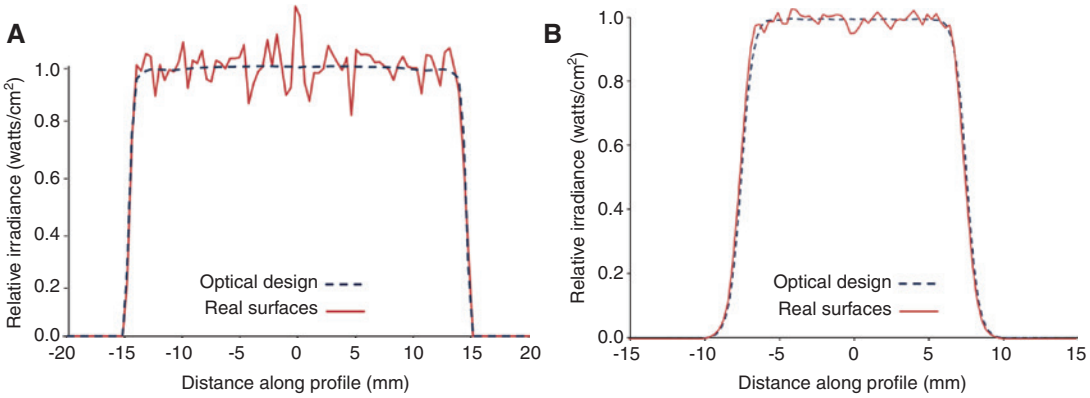

Figure 2: (Left) Intensity distribution at the working distance of WD=100 mm for Kreuzer's optical system shown in Figure 1 (top) with ideal surfaces as well as with real surfaces with slope deviations in the range of RMS$\Delta S_{2\text{-dim}}$(75 µrad/1/0.1). (Right) Intensity distribution at the working distance of WD=100 mm for our optical system shown in Figure 1 (bottom) with ideal surfaces as well as with real surfaces with slope deviations in the range of RMS$\Delta S_{2\text{-dim}}$(15 µrad/1/0.1).

systems on the market. The large distance between the aspheric surfaces leads to very small ray angles. Thus, especially the surface form and slope deviation of the aspheric surfaces have less influence on the beam profile and quality. Vice versa, creating such a short beam shaping system requires an extremely low slope deviation in the range of RMS$\Delta S_{2\text{-dim}}$(15 µrad/1/0.1) on the manufactured aspheres. Fortunately, nowadays, it is possible to manufacture such aspheric surfaces in serial production for reasonable prices, which opens up this technical realization. In other words, a higher manufacturing quality of the aspheres enables shorter overall system lengths of the beam shaping system. Figure 2 (right) shows the intensity distribution of our beam shaping system shown in Figure 1 (bottom) at the working distance of 100 mm for ideal surfaces (blue dashed line) and the simulated as-built performance of the system having real-world surfaces with slope deviations as discussed above (solid red line). The ideal surface system is very close to a perfect top-hat profile, thus keeping the very high relative RMS uniformity with the as-built performance is a perfect result. The output intensity distribution of the real surface system is rather close to ideal surface results, which was the aim of the optical design. Choosing the RMS uniformity (U_{RMS}) as performance criteria [7, 8] changes the value from 99.6% for the optical design to 97.9% for the as-built performance simulation, having an RMS variation of only 2%. In case of Kreuzer's patent, RMS uniformities of 99.2% (ideal surfaces) and 92.0% (real surfaces) were achieved.

In Figure 3, the deviation of the aspheric surface shapes from the best-fit radius is shown through the example of the particular first aspheric surfaces in the system. Having a look at the deviation, it is noticeable that the deviation of our beam shaping system is enlarged by a

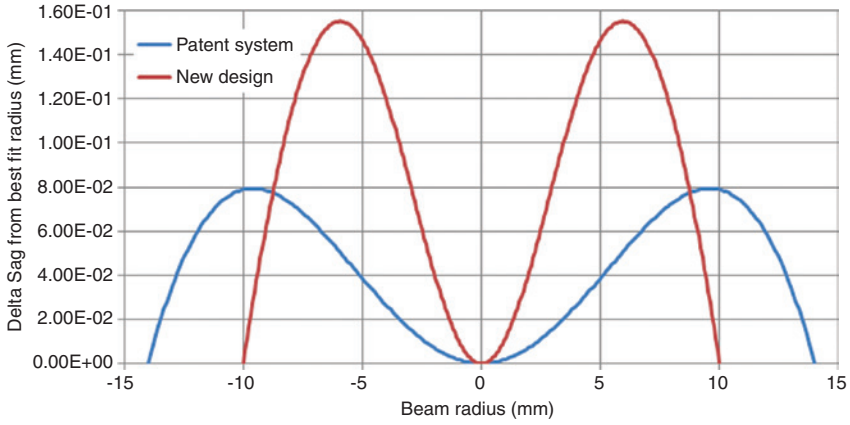

Figure 3: The deviation of the surface shape from the best-fit radius of the first aspheric lens for Kreuzer's system (blue line) and for our beam shaping system (red line).

factor of approximately 2 in comparison to Kreuzer's beam shaping system. This behavior corresponds to the fact that the overall system length of our design is half of that of Kreuzer. Due to the shorter distance between the lenses, the rays must have a larger deviation to achieve the same redistribution.

3 Scaling the entrance and exit beam diameter

Beam shaping systems work best when used with the same entrance beam profile as used within the optical design. Unfortunately, this ideal situation basically never occurs in real-world set-ups. Consequently, there are two things that have to be considered. Firstly, the optical design should be a stable solution that can handle a little change of the entrance beam diameter. Secondly, one needs to have an easy-to-handle, flexible adaption of the entrance beam to the parameters the beam shaping system works best with.

The first aspect to be analyzed is a change in input beam diameter. In general, it is important to know the input intensity distribution of refractive beam shaping systems as exact as possible, as just small deviations from the design input diameter can affect the output beam profile immediately. For the investigated system, the input beam diameter r_0 was varied up to +10% of its original size, and the resulting output intensity distributions are shown in Figure 4.

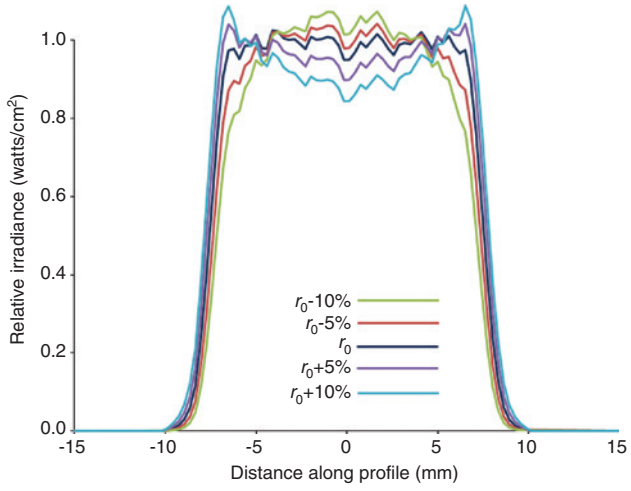

Figure 4: Output intensity distribution in dependence of the input beam diameter for the as-built beam shaping system shown in Figure 1 (bottom).

At first sight, a considerable impact of this disturbance on the beam profile is obvious. The behavior of the systems in general corresponds to the results of previous studies [9]. A smaller input beam diameter results in a bulging central region of the output beam profile, while a larger input beam diameter causes a slight depression of the central region of the output intensity distribution. However, for the shown system, the input beam diameter can vary up to ±9%. The uniformity that corresponds to this change is U_{RMS}=90.65%.

Nevertheless, setting up optical systems is simpler and much faster when a modular beam expansion system [10, 11] can adapt the beam parameters directly from the source to the beam shaping system. Due to the flexibility of the system, either a combination of SPA™ Beam Expander (Asphericon GmbH, Jena, Germany) is employed for matching the collimated laser beam to the beam shaping system (Figure 6), or a fiber-coupled source is used in combination with the SPA™ AspheriColl (Asphericon GmbH, Jena, Germany).

The SPA™ Beam Expander Kit is a monolithic solution for highly precise beam expansion. These systems take a slightly different approach than common Galilean telescope-based systems. In terms of the mode of action, they still correspond to the Galilean telescope, although they consist of only one optical element – a meniscus lens, which means both of the optically effective surfaces possess a common center of curvature. The principle has already been known for a long time; however, it leads to severe spherical aberrations in its original design with two spherical surfaces and can therefore only be used for very small incoming beam diameters and very small enlargements. Figure 5 (top) shows an example of such a lens. These kind of optical elements become very interesting when one of the two surfaces is aspherized. In line with the mode of action, this enables spherical aberration to be corrected and an afocal system to be realized, even for large incoming beam diameters. The improvement in the optical properties is clearly demonstrated in the comparison in Figure 5. The enlargement corresponds in both cases to M=2, whereby the incoming beam diameter is 10 mm.

The individual element enlargements of monolithic Galileo telescopes are relatively small due to the limitation in center thickness. However, as these are afocal beam expansion systems, they can be 'connected in series' to successively enlarge the incoming beam, one after the other in the beam course (Figure 6). This opens up completely new opportunities. With just three of these elements, one can enlarge the incoming beam by eight times, with five elements even 32 times. If only individual elements with M=2 are used, the increments of the possible enlargements

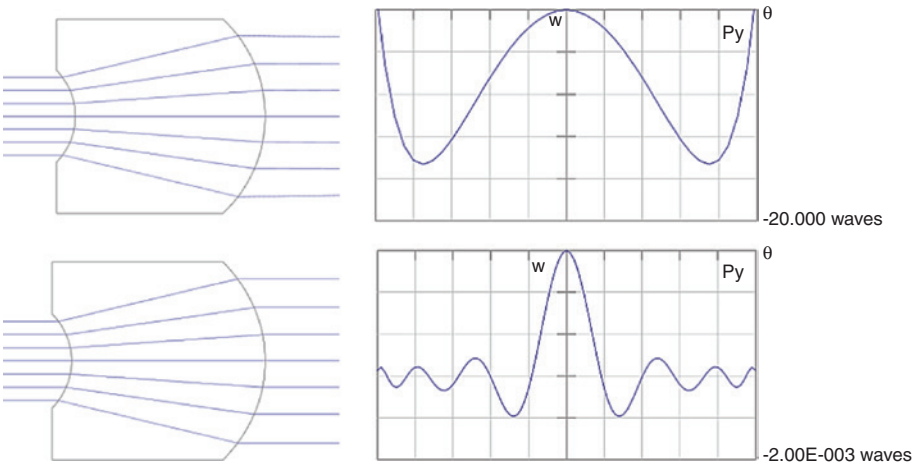

Figure 5: Two monolithic beam expansion systems are shown, (top) with spherical surfaces and (bottom) with an (convex) aspheric surface, for an enlargement of M=2. The incoming beam diameter is 10 mm. Nevertheless, the resulting wavefront aberrations for the aspheric solution are four orders of magnitude smaller.

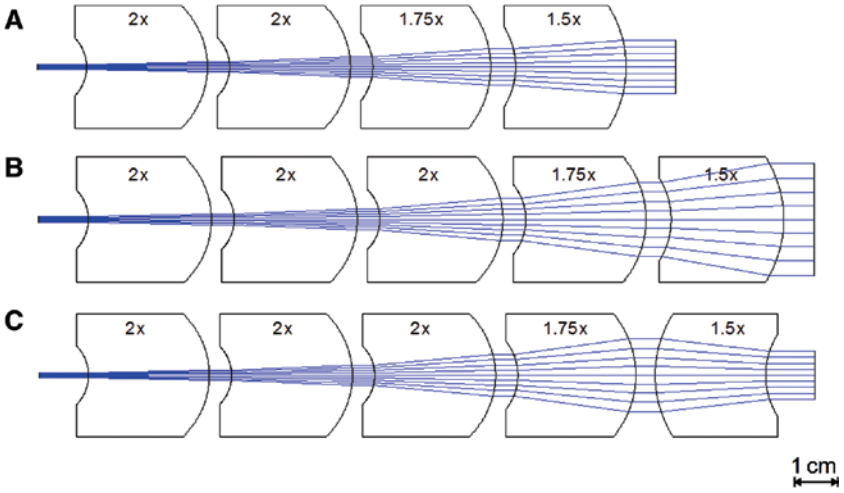

Figure 6: Three cascade systems for beam expansion based on monolithic individual systems: (A) 10.5 times enlargement, (B) 21 times enlargement, and (C) 9.3 times enlargement. The systems (A) and (B) differ by the additional element with M=2. When transferring from (B) to (C), the orientation of the last element with M=1.5 has been inverted.

are very straightforward at M=2, 4, 8, 16, 32, …. This is an optimal solution if one requires strong enlargement with minimal space used and a high wavefront quality. If, however, finer increments between the enlargement levels are desired, it is necessary to introduce other individual element enlargements, which are also very close together. Two lower levels are offered here at M=1.5 and M=1.75, especially for the version in glass. Due to the afocal dimensioning of the individual elements, the meniscus lenses can be oriented in the course of the beam either way, as shown in Figure 6C. This means, when combined, there are not only three but actually six individual element enlargements available, which significantly increases the combinatorics level. If there is one element available for each basic enlargement, this leads to 13 possibilities for the overall enlargement with just these three meniscus lenses. If one pushes these combinatorics further with additional elements, it can be seen that having up to five elements gives 230 possible combinations and therefore 230 intermediate magnifications with the largest being M=32.

The use of monolithic beam expansion systems in a cascade construction, as shown in Figure 6, involves significantly more optical surfaces than common Galilean telescope systems. What is even more, every other surface is aspheric. In order to be able to implement such a cascade system for flexible beam expansion in practice,

very high surface qualities for the individual elements are required. To prevent any restrictions on combinatorics for later use, each individual element has to be significantly better over the whole clear aperture than the 'diffraction-limited' requirement, i.e. wavefront error RMS <λ/14. For the Ti:Sa laser wavelength of 780 nm, this means an RMS wavefront error of <55 nm. For a wavelength of λ=532 nm (harmonic Nd:YAG), the RMS wavefront error is just <32 nm. If the center thickness and the decenter of the surfaces are manufactured very precisely for these requirements, this system is completely adjustment free, as all adjustment degrees of freedom are already set at an optimum as a monolithic element during manufacturing. Due to this, the attachment of additional monolithic elements to change the enlargement level can be realized completely adjustment free, and is thus quick and easy.

For demonstration of performance, Figure 7 shows measured wavefront maps of two different monolithic beam expanders with M=2 at two wavelengths (1064 and 532 nm). Taking a closer look at Figure 7 (right), one can see the diffraction-limited performance of a five-element set-up for 532 nm with M=21. This high level of wavefront quality within the beam expansion system is fundamental for good beam shaping results, as all induced aberrations corrupt the output beam quality.

Both, the SPA™ Beam Expander as well as the SPA™ AspheriColl work without further alignment of the optical elements due to the high precision mounts that can be combined effortlessly. The number of elements needed depends on the RMS uniformity (U_{RMS}) wanted. It can be minimized by employing a fiber-coupled source as there is a perfect match with just one or two SPA™ Beam Expander combined with the SPA™ AspheriColl. An example of such a set-up is shown in Figure 8. Above that, additional SPA™ Beam Expanders can be added behind the beam shaping system in order to scale the collimated

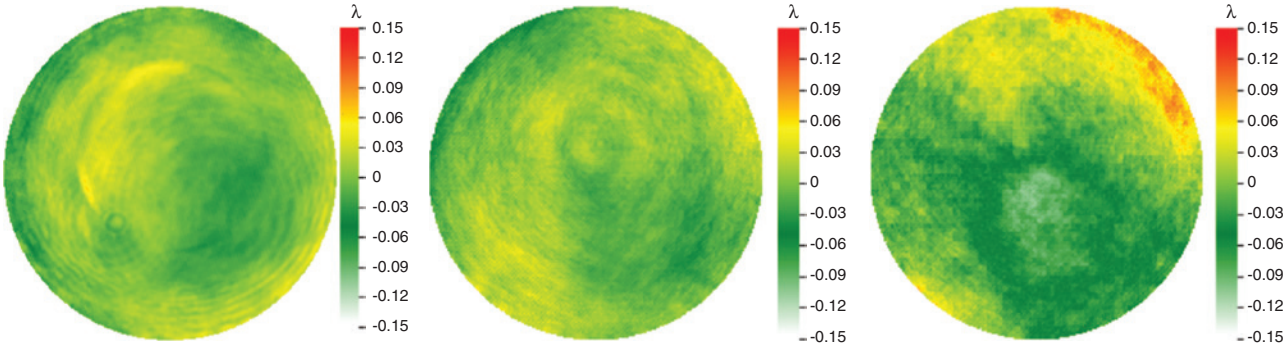

Figure 7: Measured wavefront maps of a monolithic beam expander with M=2: (left) 1064 nm, (middle) 532 nm. Having values of RMS=0.018λ, these optical elements are of very high precision and well suited for its use in a cascade system. Depicted on the right is the measured wavefront map of a five-element set of monolithic beam expanders with M=21. Having a value of RMS=0.040λ (0.220λ PV), this cascade system is performing diffraction limited.

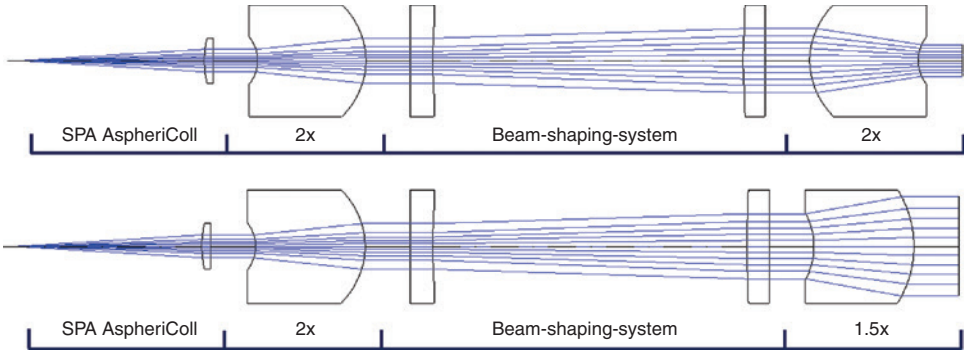

Figure 8: Adapting the input beam diameter for the beam shaping system shown in Figure 1 (bottom) by employing monolithic SPA™ Beam Expanders for, e.g. laser beams. By adding the SPA™ AspheriColl in front, a plug-and-play fiber coupling can be achieved, which needs no further adjustments. Each optical element has one aspheric surface, whose surface form deviation is extremely low, in order to achieve wavefront RMS values in the region of 20 mλ. Thus, up to five of those elements can be combined without dropping below Strehl >0.9. On the right side, an arbitrary number of SPA™ Beam Expanders can be added to scale the output diameter to the size needed for the application.

top-hat exit beam, which is the third part of this modular approach. By having just one basic beam shaping system, the achievable output beam diameter can be varied in a wide range and match exactly the application requirements. The overall length of the two systems shown in Figure 8 is about 200 mm, which is even shorter than common beam shaping systems. When installation length is an issue, this is an additional advantage next to the superior performance.

4 Beam shaping at different wavelengths

A further issue that should be considered is the wavelength behavior of the beam shaping system proposed in Figure 1 (bottom). Using diffractive beam shaping solutions, it is well known that a wavelength change of a few nanometers can easily lead to distortion of the top-hat profile. Thus, changing the application wavelength automatically requires a different beam shaping system. This lack of flexibility can be overcome with refractive approaches. The aim of the optical design was to cover a broad wavelength range in order to increase the versatility of its usage. Above that, it was a design goal to achieve this without further adjustment of the distance between the two lenses. Therefore, the impact of wavelength changes on the system's performance is analyzed. The system wavelength was varied, without matching the distance between the two lenses, in a range between 300 and 2400 nm, which represent the transmission boundaries of the chosen lens material (n=1.59, υ=61). In Figure 9, the intensity distribution for the as-built system is depicted as a function of wavelength.

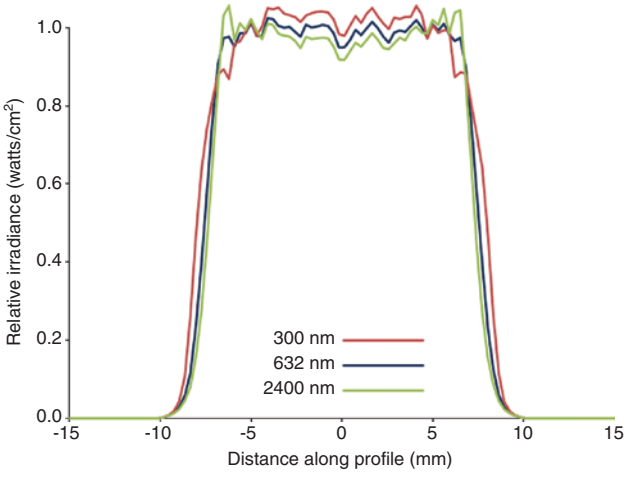

Figure 9: Output intensity distribution in dependence of the system wavelength for the as-built beam shaping system shown in Figure 1 (bottom).

In general, it is obvious that altering the wavelength does not have a significant influence on the output beam profile. The scaling of the output beam diameter is caused by the higher index of refraction for shorter wavelengths. The RMS uniformity drops <1% over the complete wavelength range. The main reason for this stable, homogenous intensity distribution is the low surface form deviation, especially the extremely low RMS slope values. Additionally, the SPA™ Beam Expander Kit offers wavelength adaption for the monolithic beam expanders as well, employing an element called SPA™ Waveλdapt (Asphericon GmbH, Jena, Germany), which is explained below. As a result, so far, the complete wavelength range from 500 to 1600 nm can be covered. Having basically no wavelength dependency, there is a huge field of applications, which can be addressed with just one optical beam shaping system for flexible and time-saving set-ups in everyday laboratory work.

Setting up a conventional beam expanding system, one can adjust the distance between both lenses to compensate for change in focal length caused by a change of wavelength. Employing monolithic elements for beam expansion as depicted in Figure 5, there is no option for compensation due to the fact that the center thickness cannot be varied. Thus, using a monolithic beam expander for another wavelength than the design wavelength, the outgoing beam is either divergent or convergent. Additionally, higher-order wavefront errors occur due to the fact that the asphere and the center thickness do not match the design intention anymore. Figure 10 depicts an example of using a shorter wavelength.

These effects become even worse when a cascade of monolithic beam expanders is used, as depicted in Figure 11. The wavefront errors add up and also divergence increases >10 times. The values stated in Figure 11 are just plain optical design. The case becomes worse when manufacturing tolerances are added in this analysis. Even though the design analysis shows a value for wavefront RMS and PtV that still works for diffraction-limited wavefront, this system cannot be expected to perform diffraction-limited in the real world.

As it is not feasible to manufacture monolithic beam expanders for each wavelength ever needed, there is a strong need for an additional component to compensate for all effects caused by a change of wavelength away from the design wavelength. The design task for this is anything but trivial. There are 230 possible combinations when having up to five elements combined, and they should be easy to use. Thus, the design goal was to create an optical

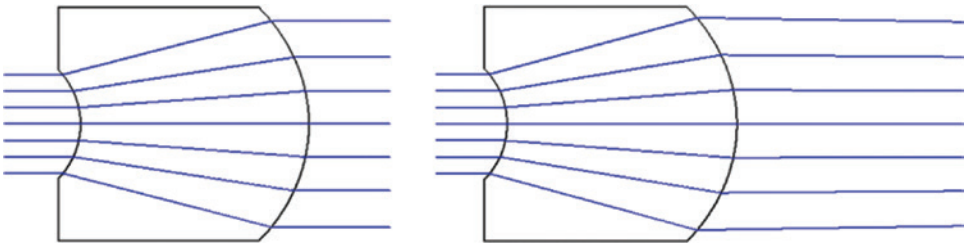

Figure 10: Two beam expanders with M=2.0. (Left) Operating at the design wavelength. (Right) Operating at a shorter wavelength than designed for.

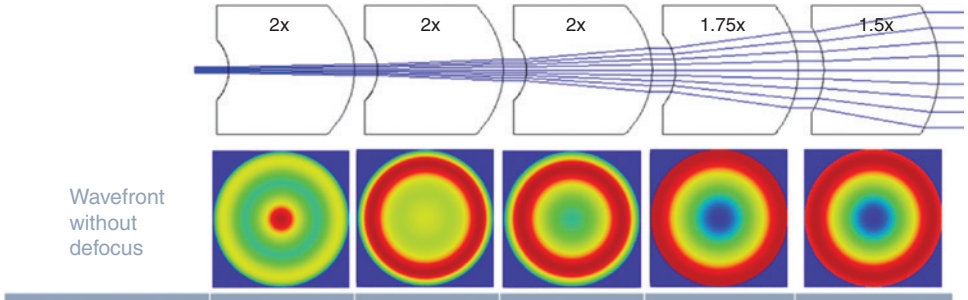

	1 BE	2 BE	3 BE	4 BE	5 BE
Divergence (μrad)	62	156	333	548	738
PtV (λ)	0 λ	0 λ	λ/330	λ/15	λ/6
RMS (λ)	0.000	0.000	0.001	0.020	0.043

Figure 11: (Top) Cascade of five beam expanders with M=21 used at 600 nm (design wavelength 532 nm). (Bottom) Wavefront, divergence, PtV, and RMS of the wavefront after passing through the given number of beam expanders.

system that is an add-on to the monolithic beam expanders that can be adjusted by minimizing the divergence of the outgoing laser beam and automatically compensates for the right amount of aberrations at that stage, while keeping the beam diameter constant. Thus, this system is a zoom lens that aims for constant magnification of 1×.

We call the resulting optical system that compensates for all effects due to change in wavelength SPA™ Waveλdapt. The working principle is kept simple on purpose to make it easy to use. When using the 'wrong' wavelength with these monolithic beam expanders, the obvious effect is a resulting divergence of the beam where it should be collimated. This is easy to detect because one can just measure the beam diameter right behind the beam expanders and then some distance away (2–4 m). After adding the SPA™ Waveλdapt to the beam expanders, it can be easily adjusted by turning one part and monitoring the change in divergence by measuring the beam diameter again until there is a match for both distances. This alignment procedure is depicted in Figure 12.

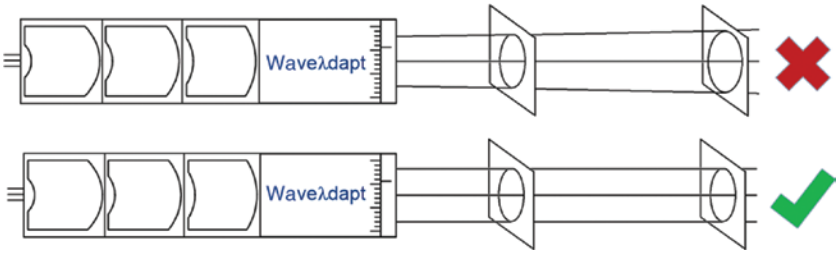

Figure 12: Alignment procedure: (top) cascade of three beam expanders combined with the SPA™ Waveλdapt used at 600 nm (design wavelength 532 nm) when the SPA™ Waveλdapt is not adjusted yet. (Bottom) Collimated beam after adjusting the SPA™ Waveλdapt for the wavelength used. Additionally, the wavefront aberrations are corrected and the wavefront is diffraction limited not in optical design only.

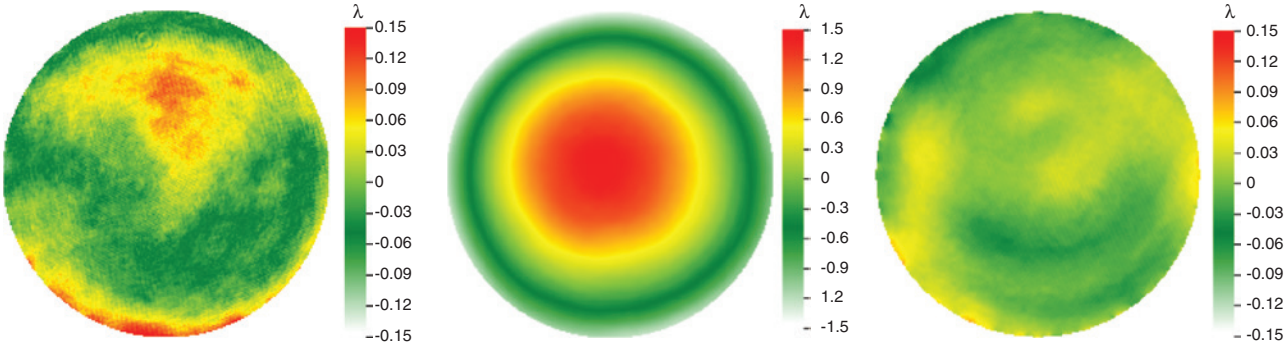

Figure 13: Measured wavefront maps of a cascade with three monolithic beam expanders with M=8. (Left) At 780 nm having RMS=0.044λ. (Middle) At 850 nm showing a defocus of 2.9λ PV (RMS=0.78λ) due to the mismatch in wavelength. (Right) Cascade with three monolithic SPA™ Beam Expanders with M=8 and SPA™ Waveλdapt at 850 nm with RMS=0.021λ. The wavefronts were measured with a Phasics high-resolution sensor (300×400 real-data points).

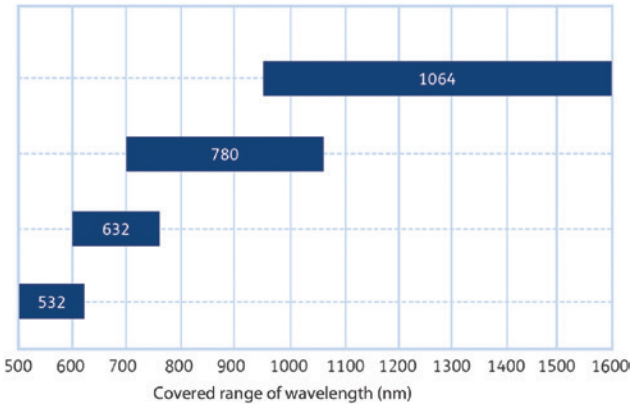

Figure 14: The spectral range covered by employing four basic sets of beam expanders at 532, 632, 780, and 1064 nm with four matching Waveλdapt.

The optical design of the SPA™ Waveλdapt is created in a way that when obtaining a collimated beam, the SPA™ Waveλdapt automatically compensates the right amount of aberrations, for the wavefront being diffraction limited in the real world, thus meaning that the theoretical values are much tighter. Thereby, the SPA™ Waveλdapt has to be placed at the position of the largest beam diameter to work as desired, which is common to color correction. Figure 13 shows examples of measured wavefronts for two different wavelengths using the 780 nm basic set of beam expanders and a SPA™ Waveλdapt. Note that these are better than diffraction limited as intended in the optical design.

Figure 14 shows a diagram of the spectral range that can be covered by designing one SPA™ Waveλdapt for each basic beam expander set (at 532, 632, 780, and 1064 nm). With this approach, it is possible to cover the complete spectral range from 500 to 1600 nm with just having four basic sets, which makes it very flexible in usage, especially as the overall length of the system is still short compared to conventional systems.

An often-used configuration is a fiber-coupled laser source, in which case the SPA™ AspheriColl is a useful solution to collimate the beam. It is applicable in exactly the same spectral range as the SPA™ Waveλdapt (Figure 14) and has also a diffraction-limited performance (Strehl >0.95).

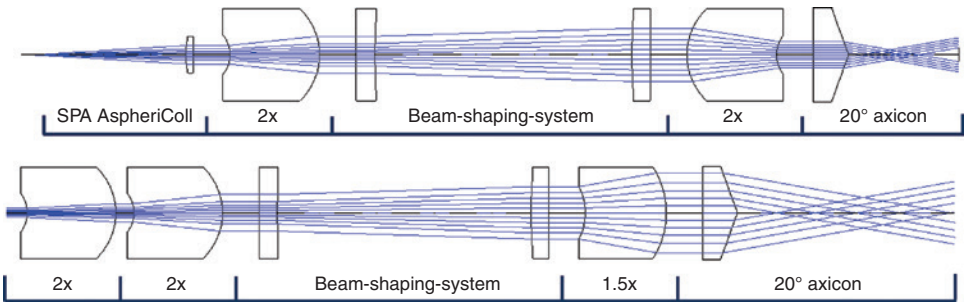

Figure 15: Example set-ups for generation of Bessel beams involving a fiber-coupled light source (top) and a laser beam adaption with 4× expansion (bottom). Note that the length of the generated Bessel beam directly depends on the beam diameter.

5 Improving the performance of other optical elements

One example of an application where a top-hat beam is extremely beneficial is the generation of Bessel beams employing axicons, as depicted in Figure 15. As discussed in Ref. [12], using beams with Gaussian intensity distribution leads to a modulation of the intensity of the central maxima along the optical axis. When a nearly constant intensity of the central peak is required, the entrance beam profile has to be a top-hat distribution. The two example set-ups shown in Figure 15 are again easily extended because the axicons are mounted within the same flexible, high-precision mounting concept – no further tilt or decenter adjustment is needed. Above that, all optical elements are interchangeable and new combination involving aspheric lenses or further axicons can be built effortlessly.

6 Conclusions

Being able to manufacture aspheric surfaces with extremely low slope deviations in serial production for reasonable prices opens up completely new fields of applications. As a direct consequence, compact optical systems such as the presented modular beam shaping system can be designed. Furthermore, combining this type of high-tech optics with high-precision mounting leads to plug-and-play solutions for experimental set-ups or even system integration. Varying input beam diameters can be handled easily as well as scaling the output beam to the optimum size for the application in hand or adding further optical elements. Finally, to emphasize the main advantage of this refractive beam shaping approach, a reliable top-hat generation over a large spectral range is possible.

References

[1] F. M. Dickey, Laser Beam Shaping: Theory and Techniques, 2nd edition (CRC Press, Boca Raton, FL, 2014).
[2] D. Hauschild, Patent US7085062B2 (August 1, 2006).
[3] B. R. Frieden, Appl. Optics 4, 1400 (1965).
[4] J. Kreuzer, US Patent US3476463 (November 4, 1969).
[5] P. W. Rhodes and D. L. Shealy, Appl. Optics 19, 3545 (1980).
[6] J. A. Hoffnagle and C. M. Jefferson, Appl. Optics 39, 5488 (2000).
[7] A. Möhl, S. Wickenhagen and U. Fuchs, in 'Proc. SPIE 9626, Optical Systems Design 2015: Optical Design and Engineering VI', 96261W (2015).
[8] A. Möhl, S. Wickenhagen and U. Fuchs, in 'Proc. SPIE 9741, High-Power Laser Materials Processing: Lasers, Beam Delivery, Diagnostics, and Applications V', 974102 (2016).
[9] J. A. Hoffnagle and D. L. Shealy, in 'Proc. SPIE 8490, Laser Beam Shaping XIII', 849004 (2012).
[10] U. Fuchs and S. Kiontke, Photon. Spectra 50 (2014).
[11] U. Fuchs and S. Wickenhagen, in 'Proc. SPIE 9580, Zoom Lenses V', 958007 (2015).
[12] T. Čižmár and K. Dholakia, Opt. Express 17, 15558 (2009).